Applied Catalysis B: Environmental 244 (2019) 576–582

Contents lists available at ScienceDirect

Applied Catalysis B: Environmental

journal homepage: www.elsevier.com/locate/apcatb

Eco-friendly prepared iron-ore-based catalysts for Fischer-Tropsch synthesis

Jae-Sung Bae[a,1], Seok Yong Hong[a,b,1], Ji Chan Park[a,b], Geun Bae Rhim[a], Min Hye Youn[a], Heondo Jeong[a], Shin Wook Kang[a], Jung-Il Yang[a], Heon Jung[a], Dong Hyun Chun[a,b,*]

[a] Clean Fuel Laboratory, Korea Institute of Energy Research, 152 Gajeong-Ro, Yuseong-Gu, Daejeon 34129, Republic of Korea
[b] Advanced Energy and System Engineering, University of Science and Technology, 217 Gajeong-Ro, Yuseong-Gu, Daejeon 34113, Republic of Korea

ARTICLE INFO

Keywords:
Fischer-Tropsch synthesis
Iron-based catalyst
Iron ore
Eco-friendliness

ABSTRACT

The iron-ore-based catalysts (IO-CAT) with catalytic properties similar to those of conventional precipitated iron-based catalysts (PFe-CAT) were successfully prepared through a combination of a wet-milling process and a wet impregnation method. This approach was much more economical and eco-friendly than a conventional precipitation technique in terms of the amounts of water and chemicals used and discharged. The IO-CAT exhibited higher surface area, a larger pore volume, and a smaller crystallite size than the unmodified iron ore samples (IO-U). In particular, the pore volume of IO-CAT was as large as that of PFe-CAT. Furthermore, the reducibility and surface basicity of IO-CAT were much higher than those of IO-U and comparable to those of PFe-CAT, which implies that a reduction promoter, Cu, and an alkali promoter, K, are used successfully to impregnate the well-developed pore structure of IO-CAT. As a result, the IO-CAT showed catalytic performance favorable for low-temperature Fischer-Tropsch synthesis (LT-FTS) using hydrogen-deficient syngas ($H_2/CO = 1$) in all aspects of CO conversion (75%), CO_2 selectivity (43 C-mol%), and C_{5+} selectivity in hydrocarbons (71 wt%). The overall catalytic performance of IO-CAT was much greater than that of IO-U and comparable to that of PFe-CAT. This strongly demonstrates new potential for economical and eco-friendly preparation of iron-based catalysts for LT-FTS.

1. Introduction

Fischer-Tropsch synthesis (FTS: $nCO + \{2n(+1)\}H_2 \rightarrow C_nH_{2n(+2)} + nH_2O$) is considered an attractive way to convert natural/shale gas, coal, biomass, and CO_2 into clean liquid fuels and high value-added chemicals via syngas ($H_2 + CO$). The FTS can be catalyzed by several transition metals such as iron, cobalt, and ruthenium, but only iron-based and cobalt-based catalysts are known to be commercially viable [1–7]. When the FTS is performed using hydrogen-deficient syngas ($H_2/CO < 2$) potentially produced via coal/biomass gasification or dry reforming of methane, iron-based catalysts are particularly advantageous for this reaction because the iron-based catalysts have additional activity for a water-gas shift (WGS: $CO + H_2O \rightarrow CO_2 + H_2$) reaction [1–3,8–10]. Furthermore, iron-based catalysts can be used for both high-temperature FTS (HT-FTS: 300–350 °C) for co-production of C_2-C_4 olefins and C_{5+} hydrocarbons, and low-temperature FTS (LT-FTS: 200–280 °C) for selective production of C_{5+} hydrocarbons [8,11]. The precipitation technique is a commercially proven method for preparation of iron-based catalysts for FTS, in particular for LT-FTS [3,8,12–15]. However, this technique requires a large amount of chemicals and water, labor-intensive procedures, and inevitable discharge of environmentally harmful waste [16,17]. Therefore, it is worth developing a new method for preparation of iron-based LT-FTS catalysts, which is eco-friendly, low-cost, and simple.

Hu et al. [16] reported that iron-based LT-FTS catalysts, which exhibit catalytic properties similar to those of conventional precipitated iron-based catalysts, can be prepared by milling metallic iron powder in a mild organic acid solution in a flow of air and subsequently drying the resulting iron oxide slurry. They demonstrated that the amount of waste water was significantly lower than for the conventional precipitation technique because, in their process, there is no residue that needs to be removed by washing the iron-oxide filtrate. However, this process may still require costly materials and generate a considerable amount of CO_2 in the drying process because an organic acid is used. Cubeiro et al. [18] reported a low-cost and eco-friendly method of preparing iron-based catalysts using iron ore as a catalyst precursor, but they used the iron-ore-based catalysts only for HT-FTS. This was probably due to the poor textural properties of the iron ore. In our previous works [19,20],

* Corresponding author at: Korea Institute of Energy Research, 152 Gajeong-Ro, Yuseong-Gu, Daejeon 34129, Republic of Korea.
E-mail address: cdhsl@kier.re.kr (D.H. Chun).
[1] These authors contributed equally to this work.

https://doi.org/10.1016/j.apcatb.2018.11.082
Received 26 July 2018; Received in revised form 23 November 2018; Accepted 27 November 2018
Available online 27 November 2018
0926-3373/

we for the first time reported the possibility of using iron-ore-based catalysts for LT-FTS. We successfully prepared iron-ore-based catalysts with enhanced textural properties by combining a wet-milling process and a wet impregnation method for use in LT-FTS. However, we have not yet reported the detailed physico-chemical properties, catalytic performance, or eco-friendliness of iron-ore-based catalysts used in our previous study, in comparison with those of conventional precipitated iron-based catalysts.

In the present study, we prepared both iron-ore-based catalysts and conventionally precipitated iron-based catalysts for LT-FTS. According to the amounts of water and chemicals used and discharged, we compared economic and environmental aspects of our new method for preparation of iron-ore-based catalysts and a conventional precipitation technique. Furthermore, we investigated the chemical composition, textural properties, crystal structure, microstructure, reduction behavior, and surface basicity to compare the two catalysts. Finally, we compared the catalytic performance of iron-ore-based catalysts to that of conventional precipitated iron-based catalysts prepared in this study and to that reported in the previous literature.

2. Experimental

2.1. Preparation of catalysts

The iron-ore-based catalysts (denoted as **IO-CAT**) were prepared by a combination of a wet-milling process and a wet impregnation method (see Fig. 1a), which are similar to those reported in our previous studies [19,20]. The coarsely ground Colombian iron ore samples, supplied by the University of Antioquia in Colombia, were used as raw iron ore samples (see Supplementary Information 1 for details). The raw iron ore samples were mixed with distilled water to form iron ore slurry for a wet-milling process. The concentration of iron ore in the slurry was about 10 wt%. The wet-milling was performed using an Ultra Apex Mill (Kotobuki model UAM-015), in a process similar to that reported in previous study [21]. The grinding vessel (0.15 L) of the Ultra Apex Mill was filled with fine zirconia beads (diameter: 0.3 mm). The beads were stirred by a vertical rotor pin (5000 rpm), and then iron ore slurry was poured into the feed vessel (1.0 L) and injected into the bottom of the grinding vessel by a feed pump. The milled iron ore slurry, which reached the top of the grinding vessel, was separated from the zirconia beads by an in-situ centrifugal separator, and the separated slurry was poured into the feed vessel again. The process was repeated continuously in re-circulation mode for 2 h. After completing the wet-milling process, the required amounts of copper (II) nitrate (Sigma-Aldrich 223395) solution and potassium carbonate (Sigma-Aldrich 347825) solution were added to the milled iron ore slurry. The mixture slurry was dried in a rotary vacuum evaporator at 50 °C, and then the dried sample was calcined in a muffle furnace at 400 °C for 4 h.

For comparison, we also prepared conventional precipitated Fe/Cu/K/SiO_2 catalysts (denoted as **PFe-CAT**) and unmodified iron ore samples (denoted as **IO-U**). The PFe-CAT were prepared through a combination of a co-precipitation technique and a wet impregnation method, in a process similar to that reported in our previous studies (see Fig. 1b) [8,12,13]. Briefly, a sodium carbonate (Sigma-Aldrich 222321) solution was added to a solution containing both iron (III) nitrate (Sigma-Aldrich 316828) and copper (II) nitrate (Sigma-Aldrich 223395) at the desired ratio at 80 ± 1 °C until the pH reached 8.0 ± 1. The precipitate slurry was washed with distilled water and filtered several times to remove undesired residues. Then, the filtrate was re-slurried in distilled water, and the required amounts of potassium carbonate (Sigma-Aldrich 347825) solution and colloidal SiO_2 (Young Il Chemical YGS-30) were added to the precipitate slurry. After drying the slurry sample in a rotary vacuum evaporator at 50 °C, the dried sample was calcined in a muffle furnace at 400 °C for 8 h. The IO-U were prepared

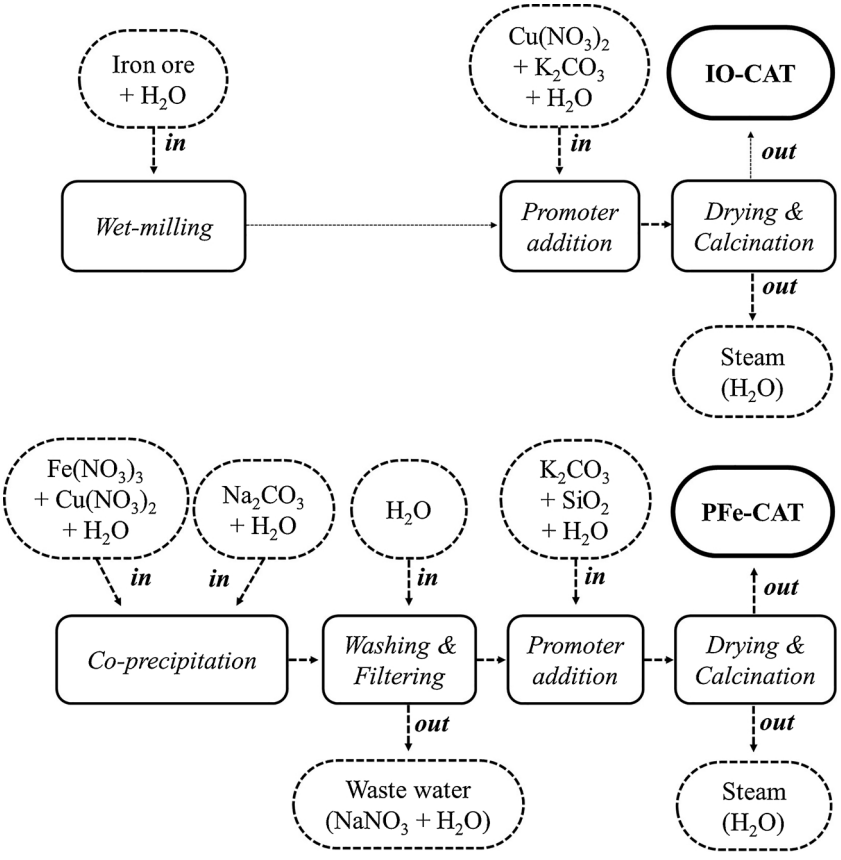

Fig. 1. Schematic diagram of the preparation procedure of (a) IO-CAT and (b) PFe-CAT.

Table 1
Summary of the amounts of water and chemicals consumed and discharged during the preparation of IO-CAT and PFe-CAT.

Sample name	Consumption ($g/g_{(cat)}$)			Discharge ($g/g_{(cat)}$)		
	Chemicals		Water	Waste water		Steam
	Nitrate	Carbonate		H_2O	$NaNO_3$	
IO-CAT	0.111	0.0331	11.6	0	0	11.6
PFe-CAT	4.16	1.91	233	223	2.74	9.84

simply by calcining the coarsely ground iron ore samples in a muffle furnace at 400 °C for 4 h. The samples to be used for catalyst performance tests were pressed into pellets and then crushed and sieved to obtain 300–600 μm particles.

The amounts of water and chemicals consumed and discharged during the preparation of IO-CAT and PFe-CAT are summarized in Table 1. It is evident that the IO-CAT requires much less nitrate and carbonate than the PFe-CAT does. Furthermore, the preparation of IO-CAT results in discharge of essentially no waste water, whereas the preparation of PFe-CAT results in the discharge of about 220 g of waste water per gram of catalyst. This clearly indicates that the new method for preparation of IO-CAT is superior to the conventional precipitation technique in all aspects: eco-friendliness, materials cost, and simplicity.

2.2. Characterization of catalysts

The chemical composition of three samples (IO-U, IO-CAT, and PFe-CAT) was analyzed by means of X-ray fluorescence spectroscopy (XRF, Rigaku ZSX Primus II). The Brunauer-Emmett-Teller (BET) surface area, the single-point pore volume, and the average pore diameter of the samples were analyzed by means of N_2 adsorption using a Micromeritics analyzer (Tristar® II 3020). The crystal structure of the samples was characterized by X-ray diffraction (XRD) with a Rigaku X-ray diffractometer (DMAX-2500) using a CuKα source. The detailed morphology of the samples was observed by means of transmission electron microscopy (TEM) using a Zeiss EM912 Omega microscope operated at 120 kV. The TEM samples were prepared by putting a few drops of the sample slurry on carbon-coated copper grids (Ted Pellar, Inc.).

The reduction behavior of the samples was analyzed by means of H_2 temperature-programmed reduction (H_2-TPR) using a BELCAT-B catalyst analyzer. After loading the samples (about 20 mg) in a sample cell, the H_2-TPR was carried out at up to 900 °C in a flow of 5% H_2 /Ar at a heating rate of 6 °C /min. The amount of H_2 consumption was measured by means of a thermal conductivity detector (TCD).

The surface basicity of the samples was analyzed by means of CO_2 temperature-programmed desorption (CO_2-TPD) using a BELCAT-B catalyst analyzer. At first, the samples (about 200 mg), loaded in a sample cell, were purged with a carrier gas, He, at 280 °C for 20 h to remove potential impurities remaining on the sample surface. After cooling the samples to 50 °C, CO_2 was fed into the sample cell for 30 min, and then the samples were purged with He for 30 min to remove weakly adsorbed species. The CO_2-TPD was carried out up to 280 °C in flowing helium at a heating rate of 6 °C /min, and the temperature was then held at 280 °C for 40 min. The amount of CO_2 desorption was measured by means of a TCD.

2.3. Fischer-Tropsch synthesis

The LT-FTS was carried out in a fixed-bed reactor composed of stainless steel (5 mm i.d. and 180 mm length), in a process similar to that described in our previous studies [8,13,19]. The catalysts (0.8 g, 300–600 μm) were diluted with glass beads (1.6 g, 425–600 μm) and then charged into the fixed-bed reactor. The catalysts were activated in situ with CO (1.4 N L/$g_{(cat)}$-h) at 280 °C under ambient pressure for 5 h. In general, CO activation is known to favor higher catalytic performance, compared to H_2 or syngas activation [22–24]. After the activation treatment, FTS was performed at 275 °C and 1.5 MPa using syngas (H_2/CO = 1.0, 2.8 N L/$g_{(cat)}$-h). The composition of the outlet gases was analyzed using an online gas chromatograph (GC, Agilent model 3000 A Micro GC) equipped with a molecular sieve and a Plot Q column. The flow rate of the outlet gases was measured by a wet-gas flow meter (Sinagawa W-NK-0.5). The composition of oil and wax was analyzed by means of an offline GC (Agilent 6890 N) with a simulated distillation method (SIMDIS, ASTM D2887) [25]. The detailed components of C_5-C_{11} hydrocarbons was analyzed by means of an offline GC (Agilent 7890B) with a detailed hydrocarbon analysis method (DHA, ASTM D6730) [26].

3. Results and discussion

3.1. Characterization of catalysts

Table 2 shows the chemical composition of IO-U, IO-CAT, and PFe-CAT. Detrimental elements such as S and Cl were not detected in the IO-U. The IO-U contains almost no Cu and K but a considerable amount of Si and Al, which are supposed to exist as SiO_2 and Al_2O_3, respectively. Therefore, we added neither SiO_2 nor Al_2O_3 as a structural promoter but did add Cu and K as chemical promoters for catalyst reduction and surface basicity, respectively. The content of Cu and K in IO-CAT was almost identical to that in PFe-CAT. Also, the chemical composition of PFe-CAT was within the range of the typical catalyst composition used in previous studies [8,12,13].

The textural properties of the IO-U, IO-CAT, and PFe-CAT analyzed by N_2 adsorption are summarized in Table 2. The pore volume of IO-U (0.096 cm^3/g) was very small due to the poor textural properties of raw iron ore samples. Therefore, the IO-U is not considered suitable for impregnating chemical promoters, Cu and K. The textural properties were greatly improved by a wet-milling process using an Ultra Apex Mill, as we reported previously [19]. Furthermore, the enhanced

Table 2
Chemical composition, textural properties, average size of crystallites, and amount of CO_2 uptake for IO-U, IO-CAT, and PFe-CAT.

Sample name	Chemical composition (g/100 g Fe) [a]							Textural properties [b]			Average size of crystallite (nm) [c]	CO_2 uptake (μmol/g) [d]
	Fe	Cu	K	Ca	P	Si	Al	BET surface area (m^2/g)	Pore volume (cm^3/g)	Average pore size (nm)	(116) of hematite (d = 1.69 Å)	
IO-U	100	–	–	3.50	2.15	6.67	4.26	47.6	0.0961	8.08	26.8	22.0
IO-CAT	100	5.28	5.43	4.12	2.01	7.70	4.88	84.7	0.312	14.7	21.5	100
PFe-CAT	100	5.25	5.09	–	–	8.77	–	135	0.326	10.8	12.5	129

[a] Analyzed by XRF.
[b] Analyzed by N_2 adsorption.
[c] Calculated by the Scherrer equation.
[d] Analyzed by CO_2-TPD.

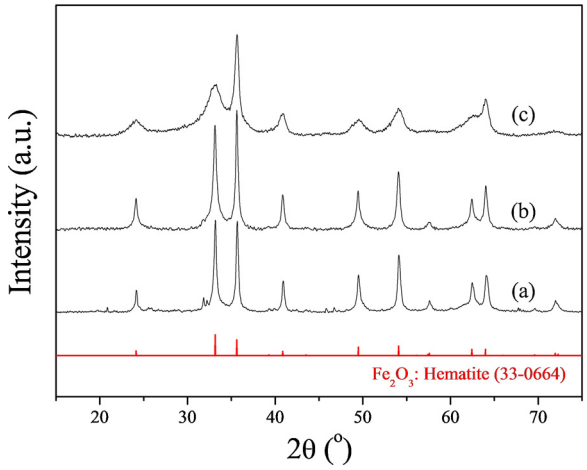

Fig. 2. XRD patterns of (a) IO-U, (b) IO-CAT, and (c) PFe-CAT.

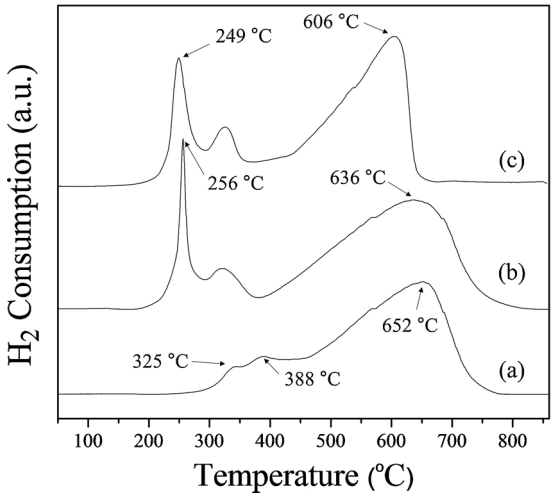

Fig. 4. H_2-TPR profiles of (a) IO-U, (b) IO-CAT, and (c) PFe-CAT.

textural properties were not deteriorated by calcination treatment at 400 °C, which implies that Si and/or Al in raw iron ore samples can play a role of structural promoters (see Supplementary Information 1 for details). As a result, the IO-CAT showed a higher BET surface area (84.7 m^2/g) and a larger pore volume (0.312 cm^3/g), than those of IO-U. The BET surface area of IO-CAT was lower than that of PFe-CAT, but the pore volume of IO-CAT was comparable to that of PFe-CAT due to its relatively large pore size. The textural properties of PFe-CAT were close to those of conventional precipitated iron-based FTS catalysts [8,14,27].

Fig. 2 shows the XRD patterns of IO-U, IO-CAT, and PFe-CAT. The XRD patterns of all samples closely matched that of hematite (α-Fe_2O_3). This indicates that siderite ($FeCO_3$) and goethite (α-FeOOH) in the raw iron ore samples [19,20] were, respectively, oxidized and decomposed to hematite during the calcination treatment at 400 °C (see Supplementary Information 2 for details). The estimated average crystallite sizes of three samples were calculated by the Scherrer equation [28], as summarized in Table 2. The average crystallite size of IO-CAT was smaller than that of IO-U, which may result in the enhanced textural properties of IO-CAT. The estimated average crystallite size of PFe-CAT was about 13 nm, which is analogous to that of typical precipitated iron-based catalysts [29–31].

The morphology of three samples was observed by TEM, as shown in Fig. 3. The TEM results corresponded well to the results of N_2 physisorption and XRD (Table 2 and Fig. 2). The TEM image of IO-U (Fig. 3a) displayed polyhedral crystallites with clear crystallite boundaries. Unlike raw iron ore samples (see Supplementary Information 3 for details) [19], small pores were observed inside some of the crystallites, probably due to the decomposition of goethite and oxidation of siderite during the calcination treatment, which generates H_2O and CO_2, respectively, and leaves pores behind. However, as revealed by N_2 physisorption (Table 2), the pores inside the crystallite are not considered numerous enough to impregnate with chemical promoters. In contrast with the TEM image of IO-U, the TEM image of IO-CAT (Fig. 3b) displayed almost no polyhedral crystallite but had irregularly shaped particles about several or several tens of nanometers in size. This means that the initial crystallite morphology in raw iron ore samples was nearly completely destroyed by the wet-milling process, generating a well-developed pore structure (Table 2). The TEM image of PFe-CAT (Fig. 3c) shows homogeneously dispersed small particles about ten nanometers in size, which is similar to the morphology of typical precipitated iron-based FTS catalysts [3,13,27].

Fig. 4 shows the reduction behavior of three samples analyzed by H_2-TPR. In the H_2-TPR profiles, the reducibility of the catalysts can be estimated by the temperatures of the H_2 consumption peaks; lower temperature indicates higher reducibility of the catalysts. The H_2-TPR profiles of iron-based catalysts can be usually divided into two stages. The first stage at 200–350 °C mainly indicates the reduction of hematite to magnetite (Fe_3O_4), and the second stage at 350–800 °C mainly indicates the reduction of magnetite to metallic iron optionally via wüstite (FeO) in the presence of structural promoters [8,12,14,32]. As shown in Fig. 4, the H_2-TPR profiles of IO-U showed a large and broad peak at about 652 °C with small shoulder peaks at about 325 and 388 °C, which is different from those of pure hematite [8,12,32], but similar to those of Fe/SiO_2 or Fe/Al_2O_3 catalysts [33,34]. This means that Si and/or Al in raw iron ore samples (Table 2) played the role of structural promoter in the TPR process, which well corresponds to the results of N_2 physisorption (see Table 2 and supplementary information 1). The H_2-TPR profiles of IO-CAT can be characterized as a

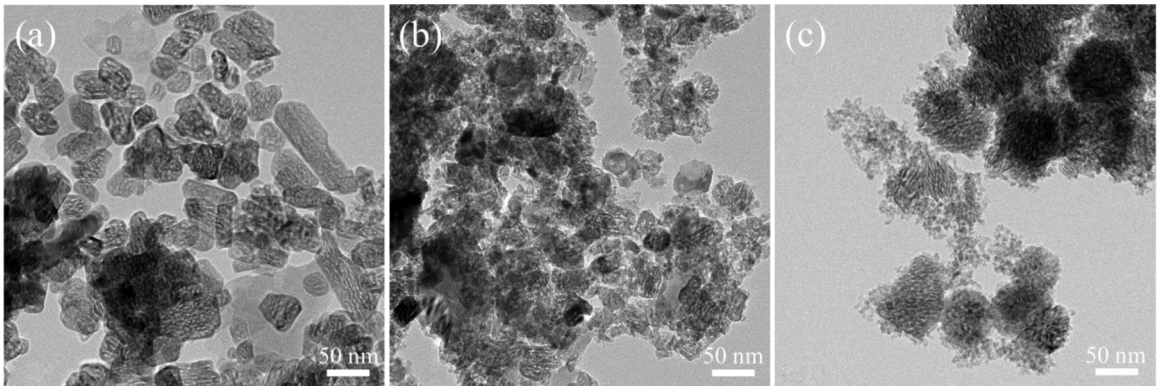

Fig. 3. TEM images of (a) IO-U, (b) IO-CAT, and (c) PFe-CAT.

combination of a sharp peak at about 256 °C and a large and broad peak at 636 °C. While the first reduction peak of IO-CAT was similar to that of PFe-CAT, the second reduction peak of IO-CAT was similar to that of IO-U. This means that the reduction of hematite to magnetite in IO-CAT was significantly improved by impregnating their enhanced pore structure with a reduction promoter (Cu). The H_2-TPR profiles of PFe-CAT were similar to those of conventional precipitated iron-based FTS catalysts [8,12,14,32]. In general, when the iron-based FTS catalysts contain no reduction promoter such as Cu and Mn, structural promoters such as SiO_2 and Al_2O_3 are known to deteriorate the reduction of the catalysts due to strong-metal-support interaction [35,36]. When the catalysts are promoted by Cu, Cu plays a critical role in determining the reduction behavior of the catalysts via a spillover of H_2 molecules from metallic Cu to nearby iron oxides [37,38]. Consequently, the intrinsic effect of structural promoters on the reduction of iron oxides becomes less significant.

The surface basicity of IO-U, IO-CAT, and PFe-CAT was analyzed by CO_2-TPD (see Supplementary Information 4 for detailed CO_2-TPD profiles). In general, the surface basicity of iron-based FTS catalysts is known to be determined by the dispersion of alkali metals because alkali metals readily donate the single electron in their s-orbital to the d-orbital of iron when the alkali metals have an effective interaction with iron. Therefore, the amount of CO_2 uptake in the CO_2-TPD profiles can be used as an efficient criterion to evaluate the surface basicity because CO_2 molecules are mainly adsorbed on the alkali surface [30,39,40]. As given in Table 2, the amount of CO_2 uptake on IO-CAT was about 4.5 times greater than that on IO-U, which means that basic sites are well developed on the surface of IO-CAT by successfully impregnating an alkali promoter (K) into the enhanced pore structure of IO-CAT. Needless to say, basic sites are essential for iron-based LT-FTS catalysts as basic sites promote the growth of -$(CH_2)_n$- chains over the catalyst surface. However, the amount of CO_2 uptake on IO-CAT was slightly less than that on PFe-CAT although the content of K in IO-CAT was almost the same as that in PFe-CAT. This can be explained by the influence of aluminum impurities, because Al is supposed to exist as Al_2O_3 in the IO-CAT. According to the previous work by Wan et al. [34], Al_2O_3 can suppress the surface basicity of precipitated iron-based FTS catalysts more strongly than SiO_2 because Al_2O_3 is a more acidic structural promoter than SiO_2 is.

3.2. Catalyst performance

The catalytic performance of IO-CAT and PFe-CAT was compared under the LT-FTS condition at 275 °C. Fig. 5 shows the CO conversion as a function of reaction time. For comparison, the result of IO-U was added to Fig. 5. The IO-U showed a low and unstable CO conversion of about 20–30%. In contrast, the CO conversion of IO-CAT exhibited a high and stable value of about 75%, which is much higher than that of IO-U and slightly lower than that of PFe-CAT. The CO conversion of PFe-CAT was comparable to the values reported in our previous studies [8,13,27].

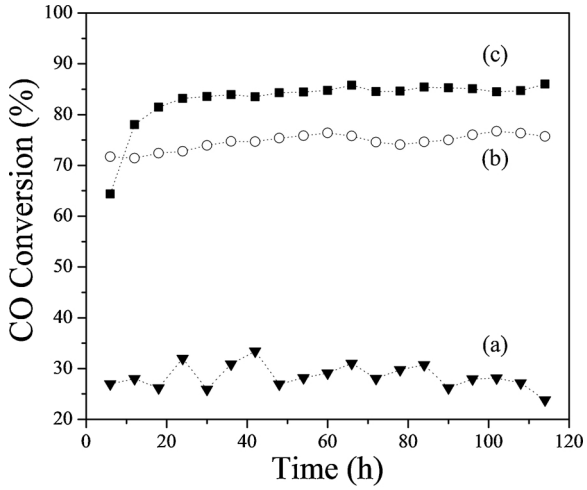

Fig. 5. CO conversion in LT-FTS as a function of reaction time: (a) IO-U, (b) IO-CAT, and (c) PFe-CAT.

Table 3
Summary of the overall catalytic performances during 66–114 h of reaction in the LT-FTS over IO-U, IO-CAT, and PFe-CAT; and the overall catalytic performance of conventional precipitated iron-based catalysts reported by other research groups.

	In this study			Previous works		
	IO-U	IO-CAT	PFe-CAT	Luo et al. (2009) [24]	Wan et al. (2006) [33]	Ma et al. (2018) [40]
Reaction condition						
H_2/CO	1.0	1.0	1.0	0.7	2.0	0.7
Temperature (°C)	275	275	275	270	250	270
Pressure (MPa)	1.5	1.5	1.5	1.3	2.0	1.3
GHSV (NL/$g_{(cat)}$-h)	2.8	2.8	2.8	3.1	2000 (h^{-1})	2.0
Catalytic performance						
CO conversion (%)	27.1	75.4	85.0	78.7	80.9	74.7
CO_2 selectivity (C-mol%)	28.9	42.6	44.2	47.5	42.2	47.7
HC selectivity (wt%)						
CH_4	20.8	9.05	9.25	36.0	10.4	5.8
C_2-C_4	41.9	20.0	22.9	(C_1-C_4)	30.4	21.8
C_5-C_{11}	21.2	30.1	17.4	37.1	32.1	72.4
(l/b in C_5-C_{11} [a])	(4.76)	(6.61)	(8.18)	–	–	(C_{5+})
(o/p in C_5-C_{11} [b])	(1.42)	(1.38)	(3.51)	–	–	
(t/i in C_5-C_{11} [c])	(0.356)	(0.954)	(22.2)	–	–	
C_{12}-C_{18}	8.45	18.0	14.3	13.9	16.6	
C_{19+}	7.69	22.9	36.2	13.0	10.5	
Mass balance (wt%)	98.8	99.5	97.2	–	–	–

[a] The ratio of linear/branched species in C_5-C_{11} hydrocarbons.
[b] The ratio of olefins/paraffins in C_5-C_{11} hydrocarbons.
[c] The ratio of terminal/internal olefins in C_5-C_{11} hydrocarbons.

Table 3 summarizes the overall catalytic performances of IO-U, IO-CAT, and PFe-CAT during 66–114 h of reaction. For comparison, the performances of precipitated iron-based LT-FTS catalysts reported by other research groups [24,34,41] were also added to Table 3. Because LT-FTS is a CO hydrogenation reaction for selective production of C_{5+} hydrocarbons, the higher CO conversion and the higher C_{5+} selectivity in hydrocarbons generally indicate the higher performance of LT-FTS catalysts. In the case of iron-based LT-FTS catalysts, moderate CO_2 selectivity, indicative of WGS activity, is also required for the use in hydrogen deficient syngas ($H_2/CO < 2$). Therefore, we focused on CO conversion, CO_2 selectivity, and C_{5+} selectivity in hydrocarbons to evaluate comparatively the catalyst performance. The IO-U showed a low CO conversion (about 27%) and low C_{5+} selectivity (about 37 wt %), which clearly indicate that the natural iron ore samples themselves cannot be used as LT-FTS catalysts. In contrast, the IO-CAT exhibited a favorable catalytic performance for all aspects of CO conversion, CO_2 selectivity, and C_{5+} selectivity in hydrocarbons. The IO-CAT showed a high CO conversion of about 75%, which is slightly lower than the value obtained in PFe-CAT (85%) and comparable to the values reported by other research groups (75–81%) [24,34,41]. The CO_2 selectivity of IO-CAT was about 43 C-mol%, which is within the range of the values obtained in precipitated iron-based catalysts (42–48 C-mol %). Furthermore, the C_{5+} selectivity of IO-CAT (71 wt%) was similar to that of PFe-CAT (68 wt%). It was also comparable to the value obtained by Ma et al. (72 wt%) [41] and even higher than the values obtained by

Wan et al. (59 wt%) [34] and Luo et al. (64 wt%) [24]. The composition of C_{5+} hydrocarbons analyzed by ASTM D2887 and ASTM D6730 is provided in Table 3. Interestingly, the C_5–C_{11} selectivity of IO-CAT (30 wt%) was much higher than that of PFe-CAT (17 wt%) while the total C_{5+} selectivity of IO-CAT was similar to that of PFe-CAT. Also, the IO-CAT exhibited the ratios of linear/branched species, olefins/paraffins, and terminal/internal olefins in C_5-C_{11} hydrocarbons lower than those of PFe-CAT. Therefore, it is inferred that the impurity Al and Si, which may exist as Al_2O_3 and SiO_2, respectively, in the IO-CAT, does not simply suppress the surface basicity but plays the role of another active site for mild hydrocracking, which involves skeletal isomerization, hydrogenation, and double bond migration. Several researchers have reported the acidic function of Al_2O_3–SiO_2 supports for various reactions [42–45]. Considering that heavy hydrocarbons such as C_{19+} hydrocarbons exist as a liquid phase in the LT-FTS condition, the retention time of heavy hydrocarbons can be longer than that of light hydrocarbons that exist as a gas phase in the reaction condition. Therefore, the acidic Al_2O_3–SiO_2 may act preferentially on heavy hydrocarbons, resulting in increased C_5–C_{11} selectivity while keeping high C_{5+} selectivity. Wan et al. [34] also reported that the C_5–C_{11} selectivity increases with an increased Al_2O_3/SiO_2 ratio when both Al_2O_3 and SiO_2 are used as structural promoters in precipitated iron-based LT-FTS catalysts.

4. Conclusions

This study reports an eco-friendly preparation of iron-ore-based catalysts that possess properties favorable for LT-FTS. We compared three types of samples: unmodified iron ore samples (IO-U), iron-ore-based catalysts (IO-CAT), and conventional precipitated iron-based catalysts (PFe-CAT). Our main results can be summarized as follows:

1) The IO-CAT, which exhibits physico-chemical properties similar to those of PFe-CAT, was successfully fabricated by a combination of a wet-milling process and a wet impregnation method. The wet-milling process efficiently broke the polyhedral crystallites in the raw iron ore. As a result, the IO-CAT showed enhanced textural properties compared to IO-U. The pore volume of IO-CAT was as large as that of PFe-CAT, which facilitates the impregnation of the IO-CAT pores with the chemical promoters, Cu and K. The successful impregnation of IO-CAT pores with Cu and K was proven by H_2-TPR and CO_2-TPD, respectively. The H_2-TPR profile of IO-CAT was much different from that of IO-U but similar to that of PFe-CAT. Also, the results of CO_2-TPD revealed that the amount of CO_2 uptake on IO-CAT was about 4.5 times as large as that on IO-U.
2) The IO-CAT showed catalytic performance favorable for LT-FTS. The performance of IO-CAT was much greater than that of IO-U. Furthermore, the overall performance of IO-CAT was comparable to that of PFe-CAT and conventional precipitated iron-based catalysts reported by other research groups. Interestingly, the C_5–C_{11} selectivity of IO-CAT (30 wt%) was much higher than that of PFe-CAT (17 wt%). We attribute the high C_5–C_{11} selectivity obtained in IO-CAT to the impurity Al and Si, which may exist as Al_2O_3 and SiO_2, respectively, in the IO-CAT. The acidic Al_2O_3–SiO_2 may act as another kind of active site for hydrocracking of heavy hydrocarbons.

Acknowledgments

This work was supported in part by the Research and Development Program of the Korea Institute of Energy Research (GP2016-0057-09/B8-2432-02) and by the National Research and Development Program of the Korea Institute of Energy Technology Evaluation and Planning (NP2015-0091/B7-3209). The authors greatly appreciate the assistance of Professors Fanor Mondragon and Angndrag Forgionny (University of Antioquia, Colombia) for supplying the coarsely ground natural iron ore samples.

Appendix A. Supplementary data

Supplementary material related to this article can be found, in the online version, at doi:https://doi.org/10.1016/j.apcatb.2018.11.082.

References

[1] R.B. Anderson, The Fischer-Tropsch Synthesis, Academic Press Inc., New York, 1984.
[2] A.P. Steynberg, M.E. Dry, Fischer-Tropsch Technology, Elsevier, Amsterdam, 2004.
[3] E. van Steen, M. Claeys, K.P. Möller, D. Nabaho, Comparing a cobalt-based catalyst with iron-based catalysts for the Fischer-Tropsch XTL-process operating at high conversion, Appl. Catal. A Gen. 549 (2018) 51–59.
[4] L. Gavrilović, J. Brandin, A. Holmen, H.J. Venvik, R. Myrstad, E.A. Blekkan, Fischer-Tropsch synthesis-Investigation of the deactivation of a Co catalyst by exposure to aerosol particles of potassium salt, Appl. Catal. B Environ. 230 (2018) 203–209.
[5] E. Jiménez-Barrera, P. Bazin, C. Lopez-Cartes, F. Romero-Sarria, M. Daturi, J.A. Odriozola, CO/H_2 adsorption on a Ru/Al_2O_3 model catalyst for Fischer Tropsch: effect of water concentration on the surface species, Appl. Catal. B Environ. 237 (2018) 986–995.
[6] C. Zhu, G.M. Bollas, Gasoline selective Fischer-Tropsch synthesis in structured bifunctional catalysts, Appl. Catal. B Environ. 235 (2018) 92–102.
[7] J. Cai, F. Jiang, X. Liu, Exploring pretreatment effects in Co/SiO_2 Fischer-Tropsch catalysts: different oxidizing gases applied to oxidation-reduction process, Appl. Catal. B Environ. 210 (2017) 1–13.
[8] D.H. Chun, J.C. Park, S.Y. Hong, J.T. Lim, C.S. Kim, H.-T. Lee, J.-I. Yang, S. Hong, H. Jung, Highly selective iron-based Fischer-Tropsch catalysts activated by CO_2-containing syngas, J. Catal. 317 (2014) 135–143.
[9] X. Yu, J. Zhang, X. Wang, Q. Ma, X. Gao, H. Xia, X. Lai, S. Fan, T.-S. Zhao, Fischer-Tropsch synthesis over methyl modified $Fe_2O_3@SiO_2$ catalysts with low CO_2 selectivity, Appl. Catal. B: Environ. 232 (2018) 420–428.
[10] C.G. Visconti, M. Martinelli, L. Falbo, A. Infantes-Molina, L. Lietti, P. Forzatti, G. Iaquaniello, E. Palo, B. Picutti, F. Brignoli, CO_2 hydrogenation to lower olefins on a high surface area K-promoted bulk Fe-catalyst, Appl. Catal. B: Environ. 200 (2017) 530–542.
[11] S. Saeidi, M. Nikoo, A. Mirvakili, S. Bahrani, N.A. Saidina Amin, M.R. Rahimpour, Recent advances in reactors for low-temperature Fischer-Tropsch synthesis: process intensification perspective, R. Chem. Eng. 31 (2015) 209–238.
[12] D.H. Chun, J.C. Park, G.B. Rhim, H.-T. Lee, J.-I. Yang, S. Hong, H. Jung, Nanocrystalline ferrihydrite-based catalysts for Fischer-Tropsch synthesis: part I. Reduction and carburization behavior, J. Nanosci. Nanotechnol. 16 (2016) 1660–1664.
[13] G.B. Rhim, S.Y. Hong, J.C. Park, H. Jung, Y.W. Rhee, D.H. Chun, Nanocrystalline ferrihydrite-based catalysts for Fischer-Tropsch synthesis: part II. Effects of activation gases on the catalytic performance, J. Nanosci. Nanotechnol. 16 (2016) 1793–1797.
[14] X. An, B. Wu, W. Hou, H. Wan, Z. Tao, T. Li, Z. Zhang, H. Xiang, Y. Li, B. Xu, F. Yi, The negative effect of residual sodium on iron-based catalyst for Fischer-Tropsch synthesis, J. Mol. Catal. A Chem. 263 (2007) 266–272.
[15] A. Halder, M. Kilianová, B. Yang, E.C. Tyo, S. Seifert, R. Prucek, A. Panáček, P. Suchomel, O. Tomanec, D.J. Gosztola, D. Milde, H.-H. Wang, L. Kvítek, R. Zbořil, S. Vajda, Highly efficient Cu-decorated iron oxide nanocatalyst for low pressure CO_2 conversion, Appl. Catal. B Environ. 225 (2018) 128–138.
[16] X.D. Hu, R. O'Brien, R. Tuell, E. Conca, C. Rubini, G. Petrini, Fischer-Tropsch catalyst prepared with a high purity iron precursor, US Patent (2007) US 7,199,077 B2.
[17] R.O'Brien, X. D. Hu, R. Tuell, Y. Cai, High temperature shift catalyst prepared with a purity iron precusor, US Patent (2006) US 7,037,876 B2.
[18] M.L. Cubeiro, M.R. Goldwasser, M.J. Perez Zurita, C. Franco, F. González-Jiménez, E. Jaimes, Mössbauer study of the evolution of a laterite iron mineral based catalyst: effect of the activation treatment, Hyperfine Interact. 93 (1994) 1831–1835.
[19] S.Y. Hong, J.C. Park, H.-T. Lee, J.-I. Yang, S. Hong, H. Jung, D.H. Chun, Nanocrystalline iron-ore-based catalysts for Fischer-Tropsch synthesis, J. Nanosci. Nanotechnol. 16 (2016) 2014–2018.
[20] D.H. Chun, J.C. Park, H. Jung, F.M. Perez, M.A. Forgionny Florez, H.-T. Lee, J.-I. Yang, S. Hong, Method for preparing iron-based catalyst and iron-based catalyst prepared by the same, US Patent (2017) US 9,789,472 B2.
[21] Y. Tanaka, M. Inkyo, R. Yumoto, J. Nagai, M. Takano, S. Nagata, Nanoparticulation of poorly water soluble drugs using a wet-mill process and physicochemical properties of the nanopowders, Chem. Pharm. Bull. 57 (2009) 1050–1057.
[22] B.H. Davis, Fischer-Tropsch synthesis: relationship between iron catalyst composition and process variables, Catal. Today 84 (2003) 83–98.
[23] R.J. O'Brien, L. Xu, R.L. Spicer, B.H. Davis, Activation study of precipitated iron Fischer-Tropsch catalysts, Energy Fuels 10 (1996) 921–926.
[24] M. Luo, H. Hamdeh, B.H. Davis, Fischer-Tropsch Synthesis: catalyst activation of low alpha iron catalyst, Catal. Today 140 (2009) 127–134.
[25] ASTM D2887-08, ASTM International, Pennsylvania, 2008.
[26] ASTM D6730-01, ASTM International, Pennsylvania, 2011.
[27] D.H. Chun, J.C. Park, H.-T. Lee, J.-I. Yang, S. Hong, H. Jung, Effects of SiO_2 Incorporation sequence on the catalytic properties of iron-based Fischer-Tropsch catalysts containing residual sodium, Catal. Lett. 143 (2013) 1035–1042.
[28] B.D. Hall, D. Zanchet, D. Ugarte, Estimating nanoparticle size from diffraction measurements, J. Appl. Cryst. 33 (2000) 1335–1341.
[29] P.A. Chernavskii, V.O. Kazak, G.V. Pankina, Y.D. Perfiliev, T. Li, M. Virginie,

A.Y. Khodakov, Influence of copper and potassium on the structure and carbidisation of supported iron catalysts for Fischer-Tropsch synthesis, Catal. Sci. Technol. 7 (2017) 2325–2334.
[30] W. Hou, B. Wu, X. An, T. Li, Z. Tao, H. Zheng, H. Xiang, Y. Li, Effect of the ratio of precipitated SiO_2 to binder SiO_2 on iron-based catalysts for Fischer-Tropsch synthesis, Catal. Lett. 119 (2007) 353–360.
[31] K.-L. Ng, K.-Y. Kok, B.-H. Ong, Facile synthesis of self-assembled cobalt oxide supported on iron oxide as the novel electrocatalyst for enhanced electrochemical water electrolysis, ACS Appl. Nano Mater. 1 (2018) 401–409.
[32] B. Wu, L. Bai, H. Xiang, Y.-W. Li, Z. Zhang, B. Zhong, An active iron catalyst containing sulfur for Fischer-Tropsch synthesis, Fuel 83 (2004) 205–212.
[33] P. Ubilla, R. Garcia, J.L.G. Fierro, N. Escalona, Hydrocarbons synthesis from a simulated biosyngas feed over Fe/SiO_2 Catalysts, J. Chil. Chem. Soc. 55 (2010) 35–38.
[34] H.-J. Wan, B.-S. Wu, C.-H. Zhang, B.-T. Teng, Z.-C. Tao, Y. Yang, Y.-L. Zhu, H.-W. Xiang, Y.-W. Li, Effect of Al_2O_3/SiO_2 ratio on iron-based catalysts for Fischer-Tropsch synthesis, Fuel 85 (2006) 1371–1377.
[35] H.-J. Wan, B.-S. Wu, X. An, T.-Z. Li, Z.-C. Tao, H.-W. Xiang, Y.-W. Li, Effect of Al_2O_3 binder on the precipitated iron-based catalysts for Fischer-Tropsch synthesis, J. Nat. Gas Chem. 16 (2007) 130–138.
[36] A. Nakhaei Pour, S.M.K. Shahri, H.R. Bozorgzadeh, Y. Zamani, A. Tavasoli, M.A. Marvast, Effect of Mg, La and Ca promoters on the structure and catalytic behavior of iron-based catalysts in Fischer-Tropsch synthesis, Appl. Catal. A Gen. 348 (2008) 201–208.
[37] S. Li, S. Krishnamoorthy, A. Li, G.D. Meitzner, E. Iglesia, Promoted iron-based catalysts for the Fischer-Tropsch Synthesis: design, synthesis, site densities, and catalytic properties, J. Catal. 206 (2002) 202–217.
[38] E. de Smit, F.M.F. de Groot, R. Blume, M. Havecker, A. Knop-Gericke, B.M. Weckhuysen, The role of Cu on the reduction behavior and surface properties of Fe-based Fischer-Tropsch catalysts, Phys. Chem. Chem. Phys. 12 (2010) 667–680.
[39] H.-J. Wan, B.-S. Wu, Z.-C. Tao, T.-Z. Li, X. An, H.-W. Xiang, Y.-W. Li, Study of an iron-based Fischer-Tropsch synthesis catalyst incorporated with SiO_2, J. Mol. Catal. A Chem. 260 (2006) 255–263.
[40] X. An, B.-S. Wu, H.-J. Wan, T.-Z. Li, Z.-C. Tao, H.-W. Xiang, Y.-W. Li, Comparative study of iron-based Fischer-Tropsch synthesis catalyst promoted with potassium or sodium, Catal. Commun. 8 (2007) 1957–1962.
[41] W. Ma, W.D. Shafer, G. Jacobs, J. Yang, D.E. Sparks, H.H. Hamdeh, B.H. Davis, Fischer-Tropsch synthesis: effect of CO conversion on CH_4 and oxygenate selectivities over precipitated Fe-K catalysts, Appl. Catal. A Gen. 560 (2018) 144–152.
[42] Y.T. Kim, K.-D. Jung, E.D. Park, Gas-phase dehydration of glycerol over silica-alumina catalysts, Appl. Catal. B Environ. 107 (2011) 177–187.
[43] P. Berteau, B. Delmon, J.L. Dallons, A. Van Gysel, Acid-base properties of silica-aluminas: use of 1-butanol dehydration as a test reaction, Appl. Catal. 70 (1991) 307–323.
[44] E. Kordouli, B. Pawelec, C. Kordulis, A. Lycourghiotis, J.L.G. Fierro, Hydrodeoxygenation of phenol on bifunctional Ni-based catalysts: effects of Mo promotion and support, Appl. Catal. B Environ. 238 (2018) 147–160.
[45] Y. Kuroda, T. Mori, Y. Yoshikawa, Improvement in the surface acidity of $AlO_2{\cdot}SiO_2$ due to a high Al dispersion, Chem. Comm. (2001) 1006–1007.